N78-10111

Contents

10. Electrification of the Proof Mass of a Drag-Free or Accelerometric Satellite

Rémy Juillerat and Jean-Pierre Philippon*
Office National d'Etudes et de Recherches Aérospatiales (ONERA)
92320 Chatillon, France
*Centre d'Etudes et de Recherches de Toulouse

Abstract

The exploitation of the data provided by the Cactus accelerometer, developed at ONERA, which makes up the payload of the D5B Castor Satellite of CNES (the French Space Agency) confirmed the existence of an electric current charging the proof mass under the influence of the magnetospheric protons, and revealed a periodic variation of this current, due to the passage of the apogee through the South Atlantic magnetic anomaly.

The paper presents the results of in-orbit measurements of this charging current, and those of calculations made for determining this current and its variations from data on proton flux at the satellite altitudes. The comparison of measured and calculated values shows that the calculation method is valid and precise enough to be used for drag-free or accelerometric satellites.

1. INTRODUCTION

A "drag-free" satellite[1] is essentially made of a proof mass protected from the surface forces acting on it and which are due to the slowing down created by the residual atmosphere as well as the various radiation pressures. The piloting system of the satellite controls the thrusters in such a way that the cage containing

the proof mass never comes into contact with it. The satellite trajectory is then in principle purely gravitational. In practice, the compensation by the thrusters of the surface forces is not perfect, the residue of compensation being due to internal perturbating forces acting on the proof mass and thus modifying the reference trajectory.

The structure of an accelerometric satellite[2] is similar, but the servo-control function takes place by the action of a force on the proof mass so that the latter is maintained in the vicinity of the cage center. The measurement of the internal forces developed by the servo-control then constitutes a measure of the sum of the surface forces acting on the satellite. The internal perturbating forces are also at the origin of the physical limitations pertaining to this type of instrument.

Electrification of the proof mass by proton and electron fluxes from the radiation belts makes up one of the main perturbations, all the more so as this electrification may increase with time and reach high levels.

So, during the definition of a drag-free or accelerometric satellite, it is important to be able to determine a priori the value that will take the current charging the proof mass in orbit so as to decide on the procedure to implement to compensate this effect.

The present paper gives the results of a comparison which has been made between this charging current as calculated for a particular orbital configuration, and the results of measurements obtained in orbit on a three-axis accelerometer (Cactus) making up the payload of the French satellite D5B-Castor.

2. PRINCIPLE OF THE DRAG-FREE AND ACCELEROMETRIC SATELLITES

Let us consider (Figure 1) a material sphere of mass m placed inside a cage fixed within a satellite. The mass of this satellite – including that of the proof mass – is M. The position of the proof mass center O_B is defined by the vector $\vec{\xi}$ in a reference frame $O_S XYZ$ linked to the satellite and such that O_S be at the center of mass of the satellite.

Let it be:

$\vec{F}_L$ the resultant of the internal forces of attraction of the proof mass by the satellite,

$\vec{F}_E$ the resultant of the surface forces acting on the satellite (atmospheric drag, radiation pressure),

$\vec{F}_P$ the thrust due to the thrusters, and

$\vec{G}_B$ and $\vec{G}_S$ the local gravitational acceleration in O_B and O_S.

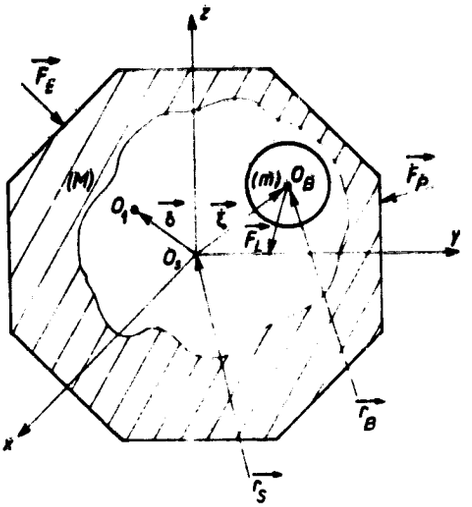

Figure 1. Drag-Free or Accelerometric Satellite Definitions

If $\vec{r}_B$ and $\vec{r}_S$ represent respectively the coordinates of O_B and O_S in an absolute frame of reference, the movements of the proof mass (m) and the satellite alone (M - m) are given by the equation of dynamics:

$$\frac{d^2\vec{r}_B}{dt^2} = \vec{G}_B + \frac{\vec{F}_L}{m} \tag{1}$$

$$\frac{d^2\vec{r}_S}{dt^2} = \vec{G}_S - \frac{\vec{F}_L}{M - m} + \frac{\vec{F}_E + \vec{F}_P}{M - m} . \tag{2}$$

2.1 Drag-Free Satellite

If we suppress any link between proof mass and cage ($\vec{F}_L = 0$), the trajectory of the proof mass is purely gravitational.

By piloting the satellite in such a way that, under the action of the thrusters, the amplitude of $\vec{\xi}$ remains at any moment lower than a value ξ_M previously chosen, we have a satellite whose trajectory can also be characterized as purely gravitational, as it only differs from that of the proof mass by a distance almost equal to ξ_M, a distance always small as compared to the satellite dimensions.

But if a perturbating force $\vec{f}$ remains between the two bodies, the true trajectory of the satellite departs from a purely gravitational trajectory and the metric

difference appearing after a time t between these two trajectories becomes equal to:

$$\Delta \left| \int_0^t \frac{\vec{f}}{m} \, dt' \, dt'' \right| . \qquad (3)$$

2 Accelerometric Satellite

Such a satellite is devoid of any propulsion means ($\vec{F}_p = 0$), but a servo-control mechanism acts on the proof mass to maintain the points O_B and O_S in a single position (within the error of the servo-control). In general, considering the smallness of the forces, no material contact should exist between proof mass and cage and the liaison force $\vec{F}_L$ is – for example – of electrostatic nature.

In these conditions $\vec{r} = \vec{r}_B - \vec{r}_S = 0$ and $\vec{G}_B = \vec{G}_S$.

Relations (1) and (2) then give:

$$\frac{\vec{F}_L}{m} = \frac{\vec{F}_E}{M} \qquad (4)$$

The acceleration imposed on the satellite by the external forces – apart from gravity – is equal to the force of proof mass-cage liaison divided by the mass of the proof mass. Thus, the measurement of this liaison force $\vec{F}_L$ makes it possible to know the resultant of external forces $\vec{F}_E$.

If an internal perturbating force $\vec{f}$ is added to the force $\vec{F}_L$ developed by the servo-control, the measure of the acceleration due to the external forces is then made false by a systematic error equal to $\vec{f}/m$.

3 PERTURBATION DUE TO THE ELECTRIFICATION OF THE PROOF MASS

In both systems that have been just described, the perturbation (of the trajectory or of the force measurement) is directly given by the acceleration $\vec{f}/m$ that the perturbating force would communicate to this proof mass alone.

These perturbating forces are of various natures and have already been the object of detailed studies[3] as well as of measurements in flight.[4, 5, 6] Among them the force provided by the defect of electric neutrality of the proof mass constitutes a perturbation that may become very important. In this case, the proof mass is subjected to an attracting force by the cage walls on which are induced electric charges whose sum is equal and of contrary sign to the charge carried by the proof

mass. Due to the spherical symmetry of the cage, this attraction is a central force around a point O_1 (Figure 1), geometric center of the cage which we try to make as near as possible of center O_S. This perturbating force $\vec{f}_E$ can be expressed by:[3, 6]

$$\vec{f}_E \quad m\beta Q^2(\vec{\epsilon} - \vec{\delta}) \tag{5}$$

where $\vec{\delta} = \overrightarrow{O_S O_1}$ and β is a coefficient defined by the geometry of the instrument.

This force is thus proportional to the square of the electric charge carried by the proof mass.

This may have two very different origins.

(1) Electrification of internal origin which appears when the proof mass leaves its contact with the cage, a contact obtained either in the presence of gravity (on the ground) or under the action of a force obtained by remote control (in orbit). This electrification is due to the charges developed either by instantaneous potentials of the various electrodes of the cage or by the differences of the work functions of the materials making up the proof mass and the cage walls.

(2) Electrification of external origin due to the accumulation of charges penetrating into the satellite, originated by the high energy particles of the radiation belts.

The first kind of electrification may be minimized by appropriate technological means. The second appears as a current charging the proof mass whose order of magnitude is hardly predictable without a detailed study. Indeed, it is very difficult to know a priori if the proof mass charge will reach a prohibitive value within a few days or few years.

Though it is necessary, during the project of a drag-free satellite or an accelerometric satellite, to foresee the adequate means for discharging the proof mass, it is highly desirable that their optimization might take into account the maximum and minimum values of the electric current that will charge the proof mass in orbit.

4. THE CACTUS D5B EXPERIMENT

The Cactus accelerometer (in French: Capteur accélérométrique capacitif triaxial ultra sensible) has been designed and built by ONERA, and made up the payload of the French satellite Castor (D5B) placed in orbit on 17 May 1975. This satellite has been built and launched by CNES (The French Space Agency) who ensured the further exploitation of the instrumentation.

1.1—Description of the Experiment

The Cactus accelerometer has a measuring range of $\pm 10^{-5}$ g on each of its three axes. The sum of internal perturbations has been evaluated before launching at 10^{-9} g. These values, as well as all the other characteristics, have been confirmed by the results obtained in orbit.[5, 7]

The core of the accelerometer is made by a proof mass in rhodiated platinum – whose mass is 550 g – placed in a cage forming with it a gap of 85 μm (Figure 2). The force linking proof mass in cage is of electrostatic nature and is obtained by means of continuous voltages applied on three systems of electrodes distributed over three orthogonal axis. These voltages are made proportional to the relative displacement of the proof mass in the cage thanks to another set of electordes realizing, on each axis, a capacitive measurement of position. The system functions by position servo-control of the proof mass and the measure of the voltages applied on the acting electrodes on each axis makes it possible, after preliminary calibration, to know the liaison force $\vec{F}_L$ and thus to determine the sum of the external forces $\vec{F}_E$ (Eq. (4)).

Figure 2. Cage, Proof Mass and Electrodes of the Cactus Accelerometer

The D5B/Cactus experiment aimed at:

(1) ensuring qualification in orbital flight of the accelerometer,[7] and

(2) providing scientific data on aeronomy.[8]

The orbit chosen was slightly excentric, with an inclination of 30°. The altitudes of apogee and perigee of the first orbit were respectively 1275 km and 277 km.

4.2 First Calculations of the Proof Mass Charging Current

At the same time as the studies for defining this experiment, theoretical and experimental studies[9, 10, 11] were performed with a view to attempt to determine the mean value of the proof mass charging current.

These works showed that:

(1) the evolution of the proof mass charge is essentially due to the bombardment of the satellite by the magnetosphere electrons and protons; and

(2) the interactions of these two types of particles with the satellite structure have widely different characteristics.

4.2.1 ELECTRONS

While crossing the materials of the satellite and the accelerometer cage, the primary electrons give rise to secondary electrons and to photons, part of which reach the proof mass and interact with it. The results are that electrons and photons circulate in both directions between proof mass and cage. The opposite fluxes of electrons are not equal, hence the existence of a charging current whose value and sign can be determined only by a detailed study.

4.2.2 PROTONS

Contrary to electrons, the protons crossing the matter do not generate secondary effects of any importance, and propagate practically in straight lines. The protons stopped within the proof mass are at the origin of a charge increase.

The work carried out at ONERA showed that:

(1) the charging current is essentially due to the primary effect of the protons stopped by the proof mass; the presumed mean value of this current has been evaluated at $+(2 \pm 1)\ 10^{-11}$ Coulomb per day; and

(2) only the electrons whose energy is about 4 MeV can give a perceptable charging current; by extrapolation above 4 MeV of the known values of the flux, the presumed electronic charging current has been evaluated at $-1.7\ 10^{-12}$ Coulomb per day, as a mean value.

At the end of this study, the expected mean value of the charging current was thus near $+2.10^{-11}$ Coulomb per day, or $2.3.10^{-16}$ ampere.

The methods used to calculate this current, as well as the assumption adopted, are described in Section 5.

4.3 Determination in Orbital Flight of the Proof Mass Charging Current

The acceleration measured by the accelerometer when the satellite is near its apogee – where the atmospheric drag is negligible – and in the shadow of the earth – where the acceleration due to the sun radiation pressure disappears – constitutes a good measure of all the internal perturbations of the instrument, as the only error

of this measurement comes from the earth radiation pressure, which provides the satellite with an acceleration of the order of 4.10^{-10} g.

The existence of a proof mass charging current is well revealed by an increase with time of this acceleration and by the returns of the latter to its bottom level during each contact between proof mass and cage, obtained by remote control. But, moreover, systematic readings of these data have also revealed time periods of about 10 days, renewed every 38 days, and during which the charging current becomes weaker.

As an illustration, Figure 3 represents the values of the modulus of the acceleration measured by the accelerometer when the satellite is at a high altitude between the 10th of May and the 20th of August 1976. We can see on this figure the periods when this current weakens: they are the periods from 18th to 31st of May, from 25th of June to 8th of July and from 28th of July to 10th of August. Outside these, the charging current takes again a higher value characterized by the increase of the measured acceleration.

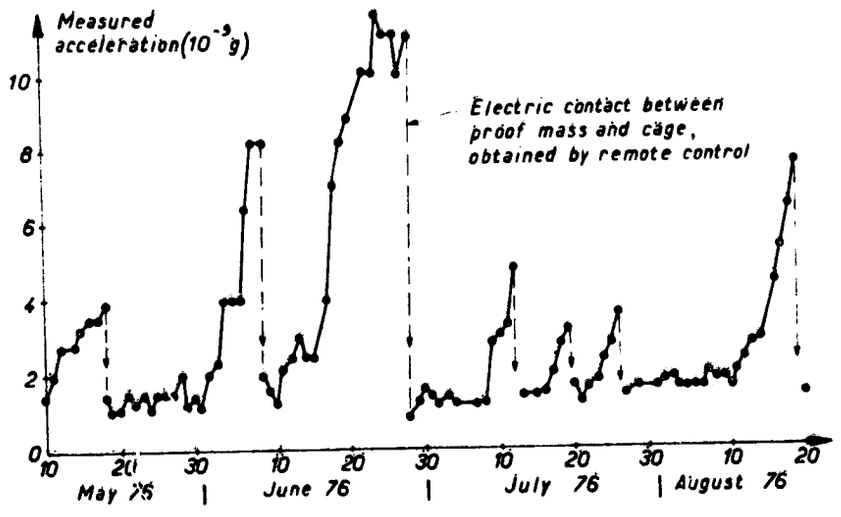

Figure 3. Acceleration Measured by Cactus at High Altitude

Various methods have been used to determine the charging current from the data transmitted by the satellite.[6, 8] These methods consist in identifying the various internal perturbations and the accelerations due to the external forces from a realistic modeling of these accelerations and by using the attitude data of the satellite. When the electric charge level becomes high enough, we consider

that the perturbation due to the charge constitutes the main term of the acceleration measured when the satellite is at a high altitude. Using Eq. (5) on the smoothed data then permits a simple but sufficiently precise calculation of Q and its time variation. For the application of Eq. (5), the knowledge of the values of β and $\vec{\delta}$ is necessary. Coefficient β had been determined on the ground before launch and has a value of $6.9.10^{17} A^{-2} s^{-4}$. The components of the $\vec{\delta}$ vector have been measured in flight by a particular manoeuvre[6]; its modulus has the value 2.16 μm.

These various methods gave coherent results which are as follows; expressed as a mean value of the charging current during the considered period of time:

-For periods with strong charging current:

. From 28th of June to 8th of July 1975: $2.1.10^{-11}$ Coulomb per day ($2.4.10^{-16}$ A)

. From 3rd to 6th of November 1975: $1.3.10^{-11}$ Coulomb per day ($1.5.10^{-16}$ A)

. From 10th to 20th of June 1976 $1.3.10^{-11}$ Coulomb per day ($1.5.10^{-16}$ A)

. From 25 August to 5 September 1976: $1.02.10^{-11}$ Coulomb per day ($1.2.10^{-16}$ A).

-For periods with weak charging current:

. From 23rd to 28th of June 1976: current lower than 5.10^{-13} Coulomb per day ($5.8.10^{-18}$ A)

. From 6th to 15th of September 1976: $1.2.10^{-12}$ Coulomb per day ($1.4.10^{-17}$ A).

5. DETAILED CALCULATION OF THE PROOF MASS CHARGING CURRENT

5.1 Interpretation of the Variations Observed on the Charging Current

We can see that the periods during which the charging current is strongly attenuated are centered on the dates when the apogee latitude is North and at its maximum value, that is 30°, a value corresponding to the orbit inclination. This important variation of the charging current may be explained by the following fact:

(1) the proton and electron fluxes decreasing rapidly with altitude, the charging current reaches a significant value only when the satellite is around its apogee; and

(2) due to the fact that the magnetic anomaly of South Atlantic which is characterized, at the altitudes where flies the satellite, by more intense particle fluxes centered over a point situated at about 25° latitude south and 40° longitude west (Figure 4), the charging current takes a high value each time the satellite flight crosses this zone.

Thus we can see that when the apogee latitude is around 30° south the satellite crosses this zone every day, while when the apogee is about 30° north this zone is avoided by the satellite.

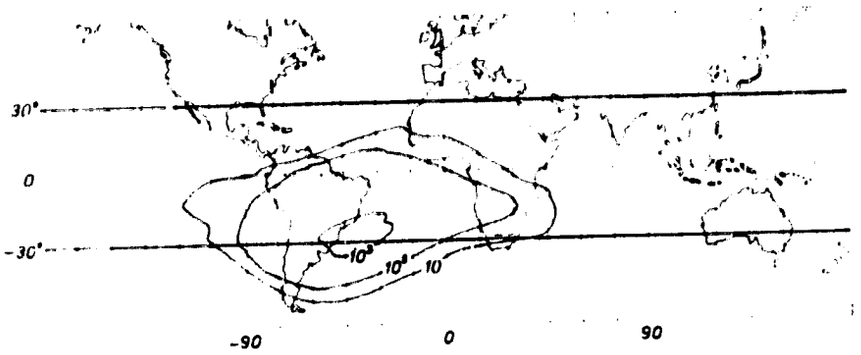

Figure 4. Proton Flux Contours -E > 100 MeV

This effect, which is a combination of the orbital movement with a geographic anomaly, is all the more marked as the orbit inclination is close to 25°, which is the case of the Castor satellite.

With a view to provide a quantitative support to this interpretation, studies previously carried out on the determination of the charging current have been repeated in order to evaluate the daily charge acquired by the proof mass during a complete-cycle of 38 days.

5.2 Calculation of the Fluxes Received by the Satellite

Since 1972, when the first calculations of the charging current have been made, the description of the radiation belt has been refined and the extrapolation of the values of electron fluxes at energies higher than 4 MeV (see Section 4.2) appeared as having no meaning. This statement confirms that only the protons in period of normal activity are at the origin of the charging current.

Two methods are usually used for evaluating a flux received by a satellite during its useful life.[12, 13] If the mission duration is long enough, the experimenter may be interested only in the mean flux and the calculation consists in determining the probability for the satellite to pass within each volume element, tabulated in energy. Here the calculation requires more precision. Indeed, a satellite in low orbit, as D5B, is subjected to an intense particle bombardment only during rather short periods which correspond to the passage through the South Atlantic anomaly.

To calculate the proof mass charging current, we must be able in each point of the orbit to estimate the flux of incident protons. Account being taken of the drift of orbital parameters, ascending node and perigee argument, a calculation of the number of protons received every 24 hr seems sufficient and remains significant. To this end, each orbit is described step by step and every minute the

geographic coordinates (altitude, latitude, longitude) are transformed into geomagnetic coordinates (B, L) that permit the consultation of the files of protons whose energies are higher 100 MeV (see Section 5.3).

Figure 5 gives as a function of time, from 3rd of June to 3rd of July, the omnidirectional mean fluxes of protons of an energy higher than 100 MeV, per square centimeter and per day, as well as the apogee latitude. The first curve illustrates well the north-south asymmetry of the radiation belt due to the South Atlantic anomaly at the altitude considered. The periodicity of this phenomenon makes it possible to extrapolate this flux curve before 3rd of June and after 3rd of July, as represented by a broken line on the figure.

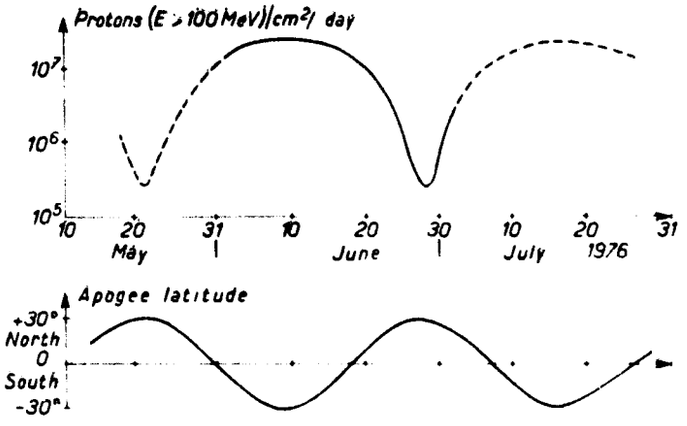

Figure 5. Isotropic Proton Flux Density Received by the Castor Satellite and Apogee Latitude at the Same Periods

5.3 Absorption of Protons by the Satellite Structure

The satellite shape is a regular polyhedron with 26 faces whose geometric center is at the center of mass and also at the center of the proof mass. A simple model of proton absorption by the satellite structure has thus been established by decomposing it into 26 equal solid angles. For each of these, the nature and the thickness of the various materials encountered by a particle moving on a straight line and reaching the center have been surveyed. Using the density of each material as a weighting parameter, these various thicknesses have then been converted in equivalent thicknesses of aluminum. These equivalent thicknesses vary from 270 mm (in a solid angle of $4\pi/13$) to 42 mm (in a solid angle of $4\pi/26$).

Moreover, the accelerometer proof mass being in platinum and having a diameter of 38 mm, the equivalent aluminum thickness corresponding to a diametral crossing of the proof mass is 316 mm.

Consequently, the proof mass charge will be due to protons whose energy is high enough to cross 42 mm of aluminum but whose energy remains lower than that necessary to cross 586 mm of the same metal.

Figure 6, taken from,[11] makes it possible to give a simple analytic formulation of the path x of protons of energy E in aluminum:

$$x = \alpha E^{-\gamma} \quad . \tag{6}$$

With x in mm and E in MeV, we obtain the following empirical values: $\alpha = 0.01$ and $\gamma = 1.73$.

Expression (6) thus permits for each solid angle of the satellite the determination of energy band of the protons which will participate in the proof mass charge. For the satellite as a whole, there are the protons whose energy is between 100 and 500 MeV which are to be considered.

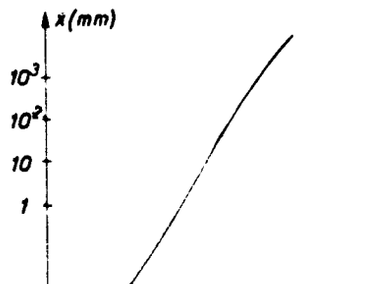

Figure 6. Proton Path in Aluminum

5.4 Calculation of the Daily Charging of the Proof Mass

The argument is that used by J. Tiffon,[11] recalled hereafter.

The flux density of protons of an energy higher than E, $\phi(>E)$, is represented by the following analytic expression:

$$\phi(>E) = k E^{-\eta} \quad . \tag{7}$$

Parameters k and η are determined empirically from the straight line which makes up a good approximation of the law representing the variation of the logarithm of the integrated flux as a function of the logarithm of energy.

As an illustration, Figure 7 represents the values of the integrated flux of protons received by the satellite during the day of 8th of June 1976, as well as the straight line giving its approximate expression.

Inside a solid angle Ω_i (Figure 8) corresponding to the previously defined dividing and for which the aluminum thickness to be crossed is x_i, the number of protons issued from a solid angle $d\omega$ and reaching the proof mass within a day is defined from Eq. (6) and (7) by:

$$d\dot{N}_{i1} \quad k\left(\frac{x_i}{\alpha}\right)^{-\eta/\gamma} R\Omega_i \cos\theta \frac{d\omega}{4\pi} \tag{8}$$

where R is the mean radius of the screen of thickness x_i. Among these, a certain quantity $d\dot{N}_{i2}$ comes out of the proof mass:

$$d\dot{N}_{i2} \quad k\left[\frac{x_i}{\alpha} + \frac{2x_r}{\alpha}\left(1 - \frac{R^2}{r^2}\sin^2\theta\right)^{1/2}\right]^{-\eta/\gamma} R\Omega_i \cos\theta \frac{d\omega}{4\pi} \quad . \tag{9}$$

In this expression, r is the proof mass radius – in platinum – and x_r its equivalent aluminum thickness.

A number of protons stopped daily by the proof mass and penetrating into the solid angle Ω_i is thus:

$$\dot{n}_i \quad \int_{\theta=0}^{\theta=\theta_o} (d\dot{N}_{i1} - d\dot{N}_{i2})$$

or, after calculation:

$$\dot{n}_i \quad \frac{r^2\Omega_i k\alpha^{\eta/\gamma}}{4}\left\{x_i^{-\eta/\gamma} - \frac{1}{2x_r^2}\left[\frac{x_i^{2-\frac{\eta}{\gamma}}}{\left(2-\frac{\eta}{\gamma}\right)\left(1-\frac{\eta}{\gamma}\right)}\right] + \frac{(x_i+2x_r)^{2-\frac{\eta}{\gamma}}}{2-\frac{\eta}{\gamma}} - \frac{x_i(x_i+2x_r)^{1-\frac{\eta}{\gamma}}}{1-\frac{\eta}{\gamma}}\right\} . \tag{10}$$

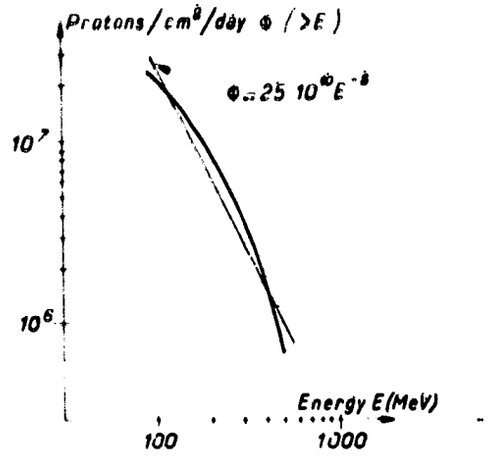

Figure 7. Proton Flux Received on June 8, 1976

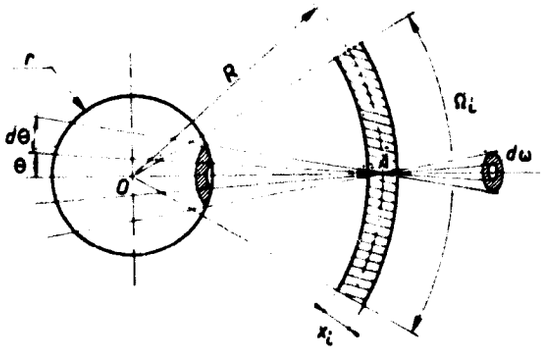

Figure 8. Method for Calculating the Proof Mass Charge

The application of Eq. (10) to each of the solid angles defined in Section 5.3 and for each day during which the radiation doses received by the satellite are characterized by the parameters k and η, permits, after summation, the calculation of the electric charge acquired daily by the proof mass.

These results are presented on Figure 9, which represents the daily charge acquired as a function of time. The abscissa corresponds to the 30 days of the month of June 1976 for which the calculation has been performed. The dates where the apogee latitude is at 30° north and 30° south have also been shown. This makes it possible to generalize the result obtained at any date of the satellite life in as much as the orbit decay is not too important.

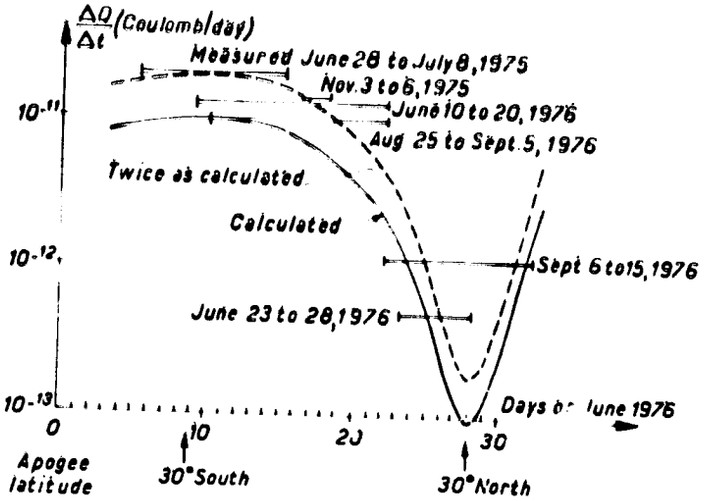

Figure 9. Calculated and Measured Values of the Charge Acquired Daily by the Proof Mass

This result obtained emphasizes well the very important variation of the charging current due to the primary effect of protons, a variation that appears as a decrease by a factor 100 when the apogee latitude is at 30^{o} north.

6. CONCLUSION

The values of the charging currents determined from the data provided by the accelerometer are also shown on Figure 9 as horizontal lines. These lines give the mean value of this current over a period corresponding to the line length. The results corresponding to July 1975, November 1975, and September 1976 are placed with the same scale but are shifted relative to the apogee latitude.

We can see that the currents, measured by this way, follow correctly the law defined by the calculated current.

On a quantitative point of view, there appears a ratio of about 2 between the measured and calculated currents. This ratio is emphasized by the broken line curve which is traced by doubling the values of the calculated currents. This coefficient 2 is not very high and may be attributed to the model of proton absorption.

Thus the results obtained confirm that it is possible, while designing the project of a drag-free satellite – or an accelerometric satellite – to determine with a sufficient precision the various values that will take the proof mass charging current as a function of orbital situations.

This evaluation should permit a better definition of the means to implement and the procedure to use to maintain the proof mass electrification to a tolerable level.

References

1. Lange, B.O. (1964) The drag free satellite, in AIAA Journal 2(No. 9):1590-1606.
2. Bernard, A., and Gay, M. (1976) Description de l'accéléromètre Cactus, in Les essais en orbite de l'accéléromètre Cactus, Publication ONERA No. 1976-5.
3. Juillerat, R. (1972) Analyse des limitations physiques des accéléromètres pour sonde spatiale et de détecteurs de sonde à traînée compensee, in International School of Physics, Varenne, Juillet 1972, Academic Press.
4. Staff of the Space Department (Johns Hopkins University, Md) and staff of the Guidance and Control Laboratory (Stanford University, Calif.) A satellite freed of all but gravitational forces: "TRIAD I".
5. Beaussier, J., Mainguy, A.M., Olivero, A. and Rolland, R. (1976) In orbit Performance of the Cactus Accelerometer. Paper presented at the XXVII International Astronautical Congress, Anaheim, Cal. Oct. 10-16, 1976.
6. Beaussier, J., and Juillerat, R. Caractérisation du seuil de l'accéléromètre Cactus, in Les essais en orbite de l'accéléromètre Cactus, Publication ONERA No. 1976-5.
7. Bouttes, J., Delattre, M., and Juillerat, R. (1976) Qualification in orbital flight of the Cactus high sensitivity accelerometer. Paper presented at the 19th COSPAR Meeting, Philadelphia, June 9-16, 1976.
8. Barlier, F., Boudon, Y., Falin, J.L., Futaully, R., Villain, J.P., Walch, J.J., Mainguy, A.M., Boudon, J.P. (1976) Preliminary results obtained from the microaccelerometer Cactus. Paper presented at the 19th COSPAR Meeting, Philadelphia, June 9-16, 1976.
9. Bourrieau, J., and Schuttler, R. (1970) Programme Eldose pour le calcul des répartitions de doses absorbées dans les écrans minces, ONERA/CERT/DERTS, NT 02/20.
10. Bourriau, J., and Schuttler, R. (1972) Transmission des électrons par les écrans plans épais, ONERA/CERT/DERTS, NT 02/24.
11. Tiffon, J. (1972) Influence des rayonnements de haute energie sur la charge électrique de la masse d'épreuve de l'accéléromètre Cactus, ONERA Technical Note No. 200.
12. Philippon, J.P. (1970) Evaluation théorique et calcul des flux de particules dans la zone stable de la magnétosphère, Thèse d'Université, Toulouse.
13. Pellat, R., and Philippon, J.P. (1976) Calcul de flux à long terme, Unpublished.